ON THE INFLUENCE OF BLADE-VORTEX-INTERACTIONS ON VORTEX STRUCTURE

B. M. J. Beesten

Department of Aerospace Engineering
RWTH Aachen, University of Technology
D-5100 Aachen, FRG

Abstract

The distortions of tip vortices because of blade-vortex-interactions (BVI) are investigated experimentally. Basic wind tunnel tests were performed to simulate BVI for the conditions of helicopter forward flight. For the interaction with rotor blades, a strong vortex was generated as tip vortex of a special wing arrangement. The relative position between rotor and interacting vortex could be varied by moving the wing system. Two kinds of investigations were carried out: a flow visualization technique to obtain the deformations of the vortex trajectory and velocity measurements, using split fiber probes, to estimate the influence of BVI on the axial and tangential velocity profiles of the vortex. For investigating the influence of vortex strength and structure, tests with different vortices were conducted.

The results of the various tests are presented and some basic explanations of the observed phenomena are given. As a main result, it was found that, under certain conditions, the vortex trajectory was turned into a corkscrew or spiral shape. The influence of various parameters on the geometry of the spiral is presented. Concerning the velocity profiles, the maximum tangential velocity and the axial velocity defect are of special interest. For very close interactions, the flow visualization shows a vortex bursting in form of a short spiral. A special investigation of this bursting is planed for the future.

Nomenclature

A	amplitude
c_R	chord of rotor blade
c_W	chord of vortex generating wing
R	rotor radius
r	radial position
r_c	vortex core radius
s	dimensionless span position
t	time past interaction
V_{ax}	axial velocity
V_{tan}	tangential velocity
V_∞	freestream velocity
x, y, z	Cartesian coordinates
x_v	lateral vortex position
z_v	interaction distance
α	angle of attack
α_{TPP}	rotor plane angle of attack
γ	angle of deflection
Γ_b	blade-bound circulation
Γ_v	vortex circulation
Γ_0	maximum blade-bound circulation
δ	axial velocity defect
λ	wave length
μ	advance ratio
ϑ_R	collective pitch angle of rotor
Ψ	rotor azimuth
Ω	rotor rotational speed

1. Introduction

Helicopter aerodynamics are mainly dominated by unsteady effects. Among these effects, blade-vortex-interactions (BVI) of tip vortices with rotor blades (Fig. 1) play a major role because of the emission of high impulsive noise and the generation of dynamic blade loads. Therefore, BVI is at present a main subject of helicopter research.

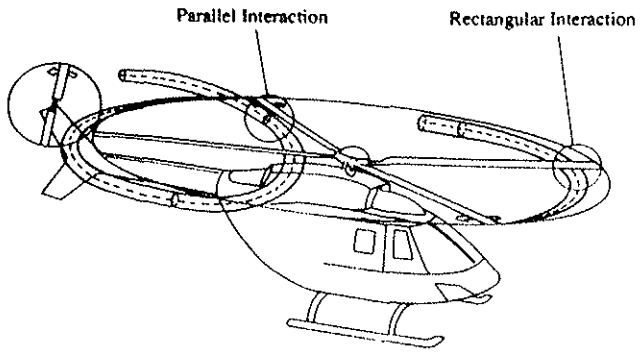

Fig. 1 BVI of different type

Incorporated in a research program on helicopter noise reduction, several experiments on BVI were conducted at the RWTH Aachen, University of Technology, since 1981 (Ref. 1, 2). Within this program, also theoretical models and computer codes were developed in order to

calculate rotor flow, tip vortex strength and position, unsteady blade loads and noise emission.

The intention of this paper is to understand the effects of BVI which cause a deformation of the vortex path and a modification of the vortex structure. The knowledge of these effects seems to be important because the distorted vortex segments may interact several times with the main rotor blades as well as with the tail rotor blades. In some tests even a vortex bursting was observed, an effect which increased the interest in appropriate investigations. Since there are nearly no significant publications on this subject, some basic wind tunnel tests were performed for analyzing the influence of the governing parameters.

To simplify the BVI for a helicopter in forward flight, it was decided to generate the interacting vortex by an external vortex generating device. This experimental setup was chosen because vortex location, structure and strength are easy to control and to measure before and after the interaction. There is a remarkable amount of experience with comparable setups in the team (Ref. 1) and other scientists also used such methods successfully (Ref. 3). The own tip vortex system of the main rotor also exists, but it is expected that it has at most for lifting rotors a notable influence on the investigated phenomena.

2. Experimental setup

2.1. Vortex arrangement

The interacting vortex was generated by a special arrangement of fixed wings. Normally, the structure of wing tip vortices may be different from that of a main rotor tip vortex, which has a small core radius and is highly concentrated. To model a main rotor tip vortex, a special vortex generator was built (Fig. 2), which permitted some variations like using 1 to 4 wings to merge their tip vortices in the center, using different wing shapes, varying the angle of attack and the distance between the wing tips. The generator was fitted in front of the 1.5 m diameter wind tunnel nozzle and could be moved in vertical and horizontal direction. The wings had a 0.1 m chord with a NACA 0015 profile and no twist.

A large number of vortices were investigated. Their tangential and axial velocity profiles were measured by split fiber probes and constant temperature hot wire anemometers to select the vortices which are most helicopter-like. Special chord extensions at the trailing edge of the generator wings have been adapted for creating a suitable spanwise circulation distribution at the wings (Fig. 3). As a result, two vortices (vortex 1 and vortex 2 in table 1) were selected as basic vortices with small symmetric cores combined with a high strength (Fig. 4).Their main difference was the amount in axial velocity defect δ (Fig. 4b). The circulation distribution of these vortices showed acceptable agreement with the helicopter vortex model of Ref. 4 (Fig. 5).

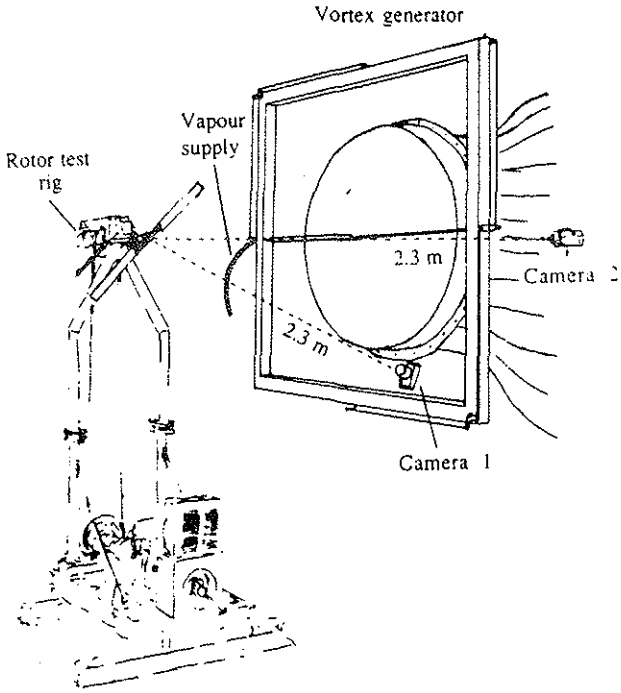

Fig. 2 Test facility

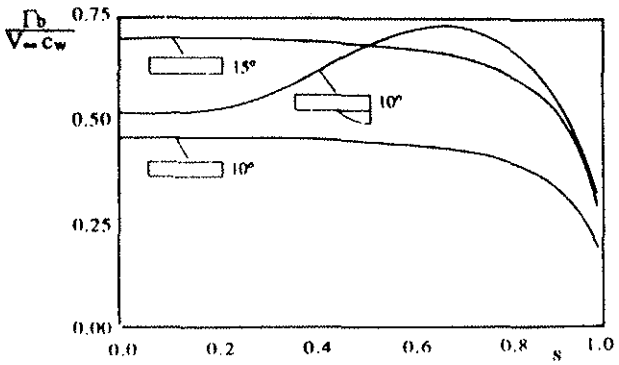

Fig. 3 Bound circulation distribution

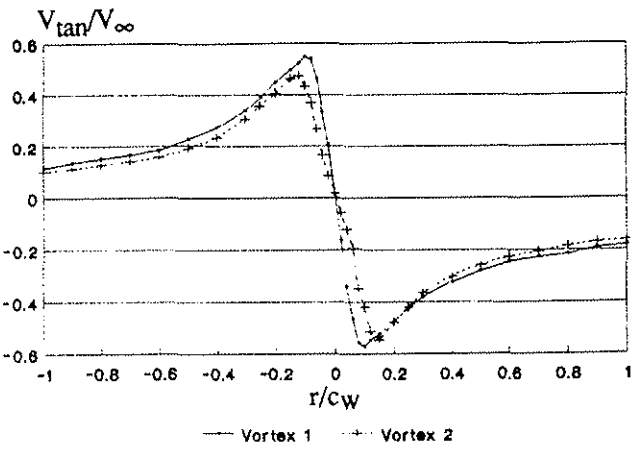

Fig. 4a Tangential velocity profile

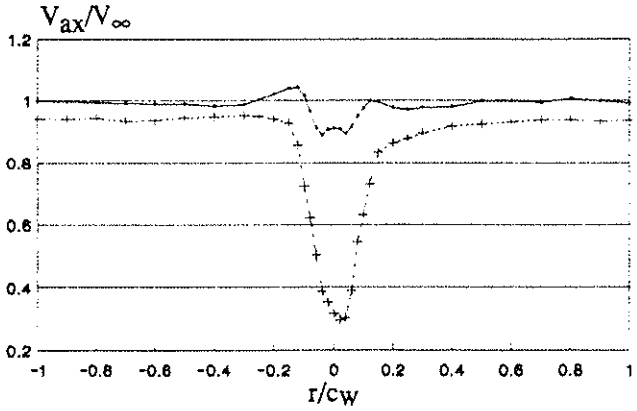

Fig. 4b Axial velocity profile

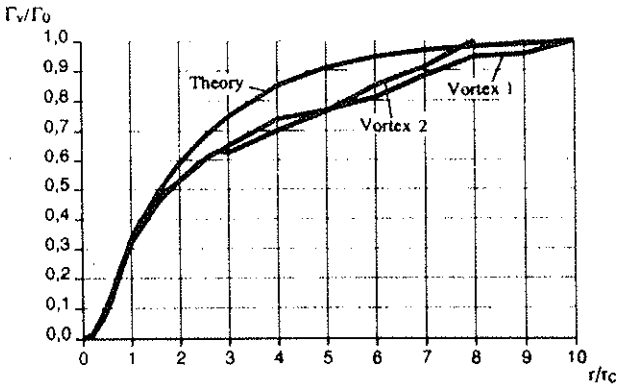

Fig. 5 Vortex circulation distribution

To analyze the influence of the vortex strength, two further vortices were used in some test runs (vortex 3 and vortex 4 in table 1).

Tab. 1 Investigated vortices

	α	Chord ext.	$\Gamma_v/V_\infty c_w$
Vortex 1	10°	yes	0.94
Vortex 2	15°	no	0.83
Vortex 3	8°	yes	0.69
Vortex 4	10°	no	0.74

Here, α is the angle of attack of the vortex generator wings. Applying the theory of Leibovich (Ref. 5,6) on the measured profiles of the tangential and axial velocities of the vortices, it turned out that vortex 2 should be unstable while the other vortices are stable.

2.2. Rotor test facility

Following these vortex measurements, a model rotor was installed in the open test section of the wind tunnel. It was a two-bladed rotor of 1.05 m diameter equipped with collective and cyclic pitch control. The untwisted blades had a NACA 0015 profile with a chord length of 0.054 m and were made out of glass fiber composite.

The distance between the generator wing trailing edge and the blade tips (at $\psi = 180°$) was set to 1.15 m to ensure that the vortices of the generator have merged and rolled up completely. The rotor plane was adjusted parallel to the wind tunnel flow direction ($\alpha_{TPP} = 0°$) and the rotor was operated with zero cyclic pitch.

2.3. Measurement setup

Two kinds of investigations have been carried out:

- a flow visualization technique for observing the influence of BVI on the vortex trajectory and
- velocity measurements, using split fiber probes, to obtain the changes in vortex velocity distributions after BVI.

To visualize the vortex trajectory, vapor was emitted from the tips of the vortex generator wings. For measuring the displacements of the vortex center, simultaneous photographs of the visualized vortex core were taken from the side view and a downstream view (Fig. 2). In addition to that, stroboscopically flashed video recordings were taken simultaneously. For analyzing the photographs, a digital image processing unit was used. By extracting the center of the vapor filaments (line with less vapor for example in Fig. 7), the positions of the vortex core were obtained and could be analyzed.

Velocity measurements, using a split fiber probe (DANTEC 55 R 55) and a constant temperature anemometer, were made with and without the influence of the rotating rotor downstream of the generator wings at several planes normal to the wind tunnel flow direction. The velocity data were digitized and stored on-line on a micro computer. A number of values was accumulated and averaged. Without running the rotor the vortex position showed only negligible fluctuations, so that it was concluded that this averaging process could be applied for the undisturbed vortex. But, when BVI occurred, the center of the vortices winds up to a spiral. This phenomenon demanded a special measuring procedure where the velocity data had to be triggered by the rotor revolutions. In this way up to 30 triggered values have been collected and averaged to get one velocity. The probe position was computer controlled and the measured axial and tangential velocities were plotted automatically versus the position.

3. Results

3.1. Vortex trajectories

At the measurements, the influence of several parameters was investigated. So, rotor rotational speed, wind tunnel velocity and vortex strength were varied. Measurements with a non lifting rotor (zero collective angle) and a lifting rotor (collective pitch of 5° and 10°) were performed. As Fig. 6 shows, tests were conducted for two distances x_V in lateral direction. For x_V=0 the vortex trajectory is parallel to the leading edge of the interacting blade, which is called parallel interaction; x_V=-0.6R is an example of an oblique interaction where in this case the angle between the leading edge of the blade and the vortex is about 50°. In all cases, the interaction distance z_V between the rotor area and the vortex was enlarged in steps until no distortion could be recognized anymore. Measurements with the vortex located above the rotor (z_V negative) were conducted currently only up to an interaction distance of 0.37 c_R. A survey of the parameter variations gives Tab. 2.

To restrict the number of combinations, two reference tests (No. 1 and No. 4 in Tab. 2) were chosen to which all parameter variations were related. Choosing an advance ratio of 0.4 as standard, gave more time to observe the fluctuations before a second interaction took place.

Tab. 2 Parameter variation

Test No.	Vortex No.	V_∞	rpm	μ	υ_R	x_V
		m/s	min^{-1}		°	m
1	1	20	918	0.4	0	0
2	1	20	1377	0.3	0	0
3	3	20	918	0.4	0	0
4	2	20	918	0.4	0	0
5	4	20	918	0.4	0	0
6	(2)	10	918	0.2	0	0
7	(2)	30	1377	0.4	0	0
8	2	20	918	0.4	10	0
9	2	20	1377	0.3	10	0
10	1	20	918	0.4	10	0
11	1	20	1377	0.3	10	0
12	1	20	918	0.4	5	0
13	1	20	918	0.4	10	0.3
14	1	20	1377	0.3	10	0.3
15	1	20	918	0.4	0	0.3
16	2	20	918	0.4	10	0.3

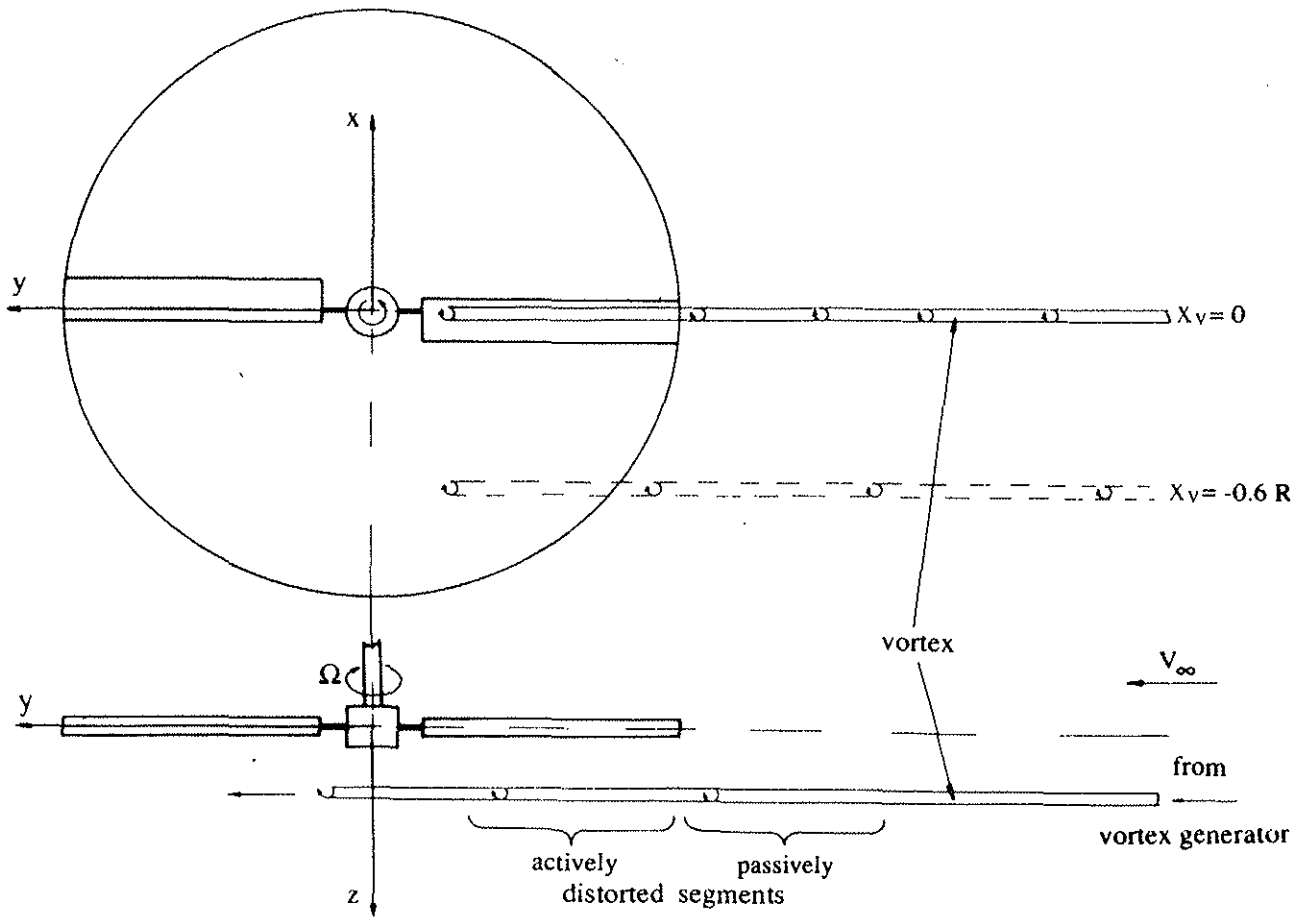

Fig. 6 Interaction geometrie

As the first step of analyzing the test results, the video and photographic pictures were used to get a qualitative survey of the trajectory deformation. It was found that in all test cases the straight vortex trajectory was more or less turned into a spiral or corkscrew shape due to BVI (Fig. 7). It is remarkable that the spiral was extended to those parts of the vortex which had no direct interaction with the blade ('passively distorted' segments, see Fig. 6), even if the hit of the blade mainly destroyed the 'actively distorted 'vortex segments.

It was found that the spiral form was flattened in case of an oblique interaction. That means that the amplitude of the motion is bigger normal to the rotor area than parallel to it, which gives the spiral an elliptical cross section. Fig. 8 shows a typical visualization of such a 'flat spiral'.

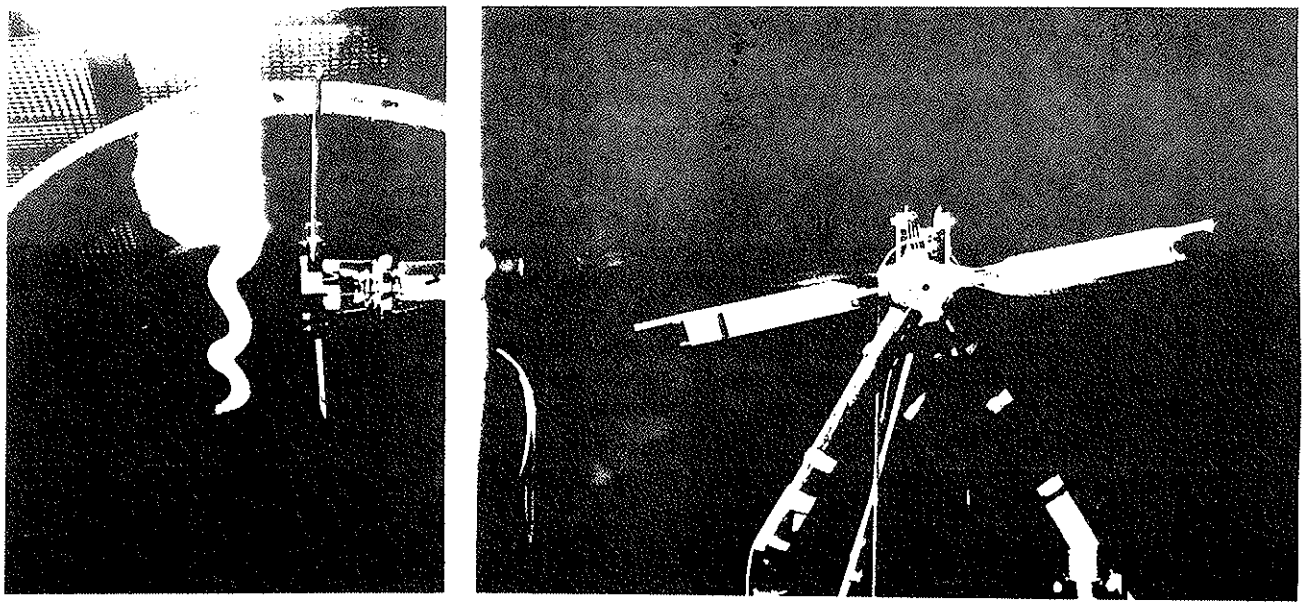

Fig. 7 Vortex spiral

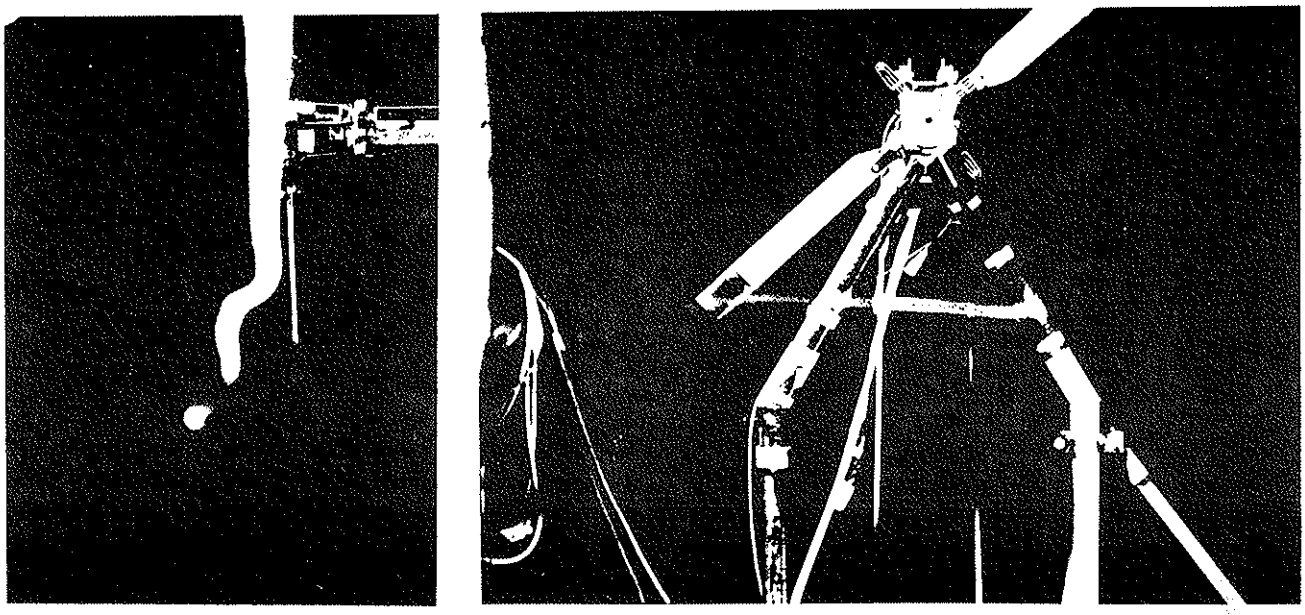

Fig. 8 'Flat spiral'

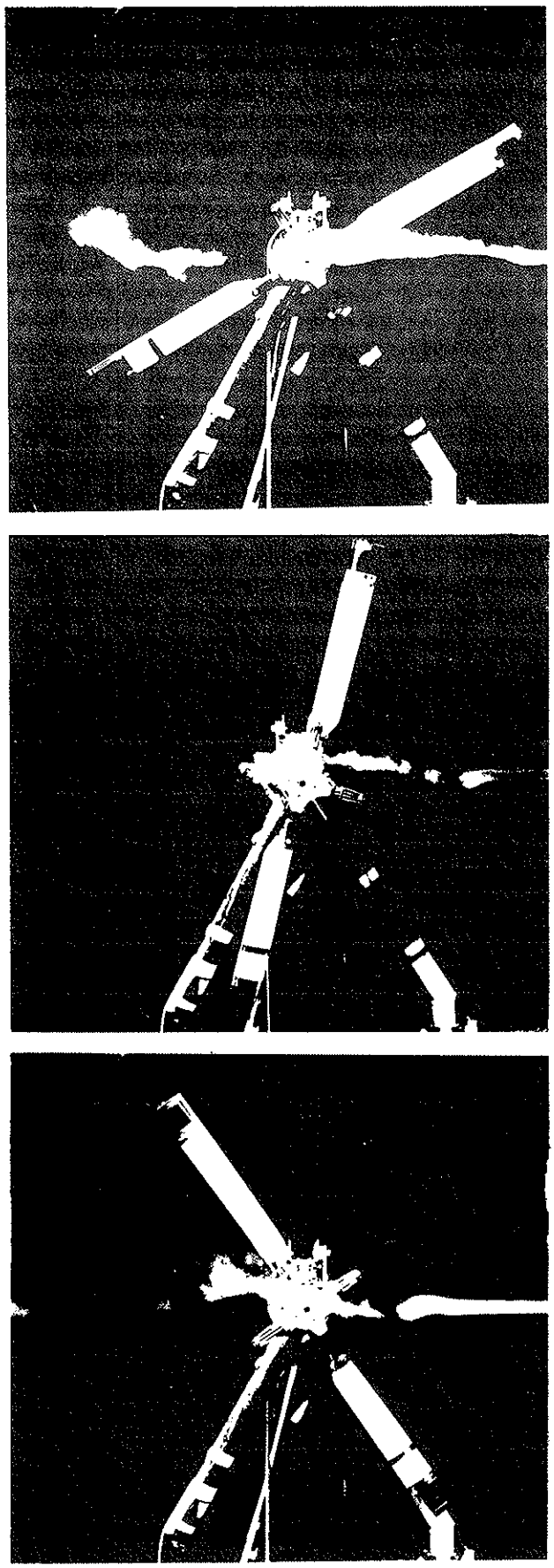

Fig. 9 Spiral growing

For parallel interactions of vortices passing below (downstream) the rotor, it was found that the actively distorted segments were moved in the direction of the rotating blade motion. Fig. 9 shows in its upper part an example of this displacement, which is followed by the beginning spiral formation. But, for vortices passing above the rotor, the actively distorted segments showed a movement against the rotation. An explanation for that behavior is illustrated in Fig. 10 for the non-lifting case. The interacting vortices rotate anti-clockwise according to the experimental setup. In the beginning of the BVI (blade position 1) the vortices induce positive angles of attack at the passing blade. That causes a variation of the bound vorticity at the blade as marked in. When the blade has passed by (blade position 2), the vortices induce negative angles of attack causing a bound vorticity in the opposite direction to that of blade position 1. This phenomenon is the same for the vortex passing above or below the blade. The variation of bound vorticity generates a trailing vortex sheet which induces velocities at the position of the interacting vortices. This leads to a movement of the vortices, whose direction is shown in Fig. 10. If the rotor blades are generating lift, the described phenomena are principally the same.

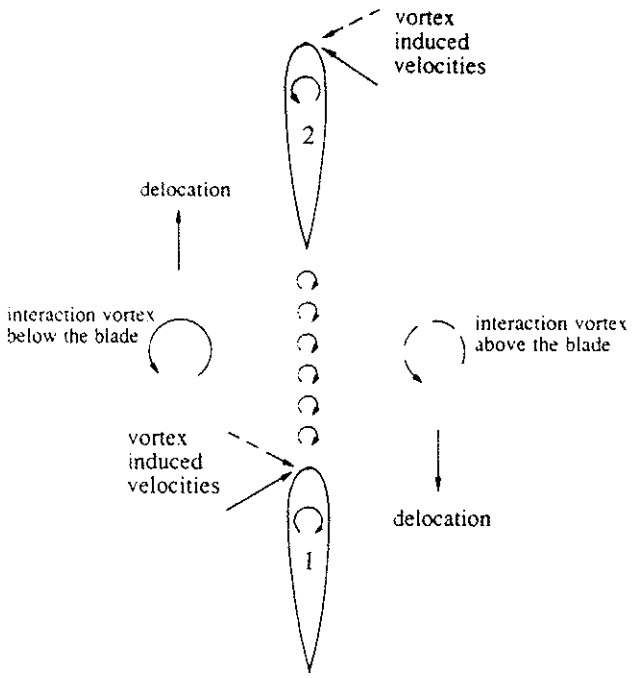

Fig. 10 Vortex delocation

It is an important point, that this induced displacement of the interacting vortex was the starting point of a forced meandering motion in form of a spiral. The spiral was caused by self-induction; every segment of the vortex induced velocities mainly in radial direction at the position of each other segment.

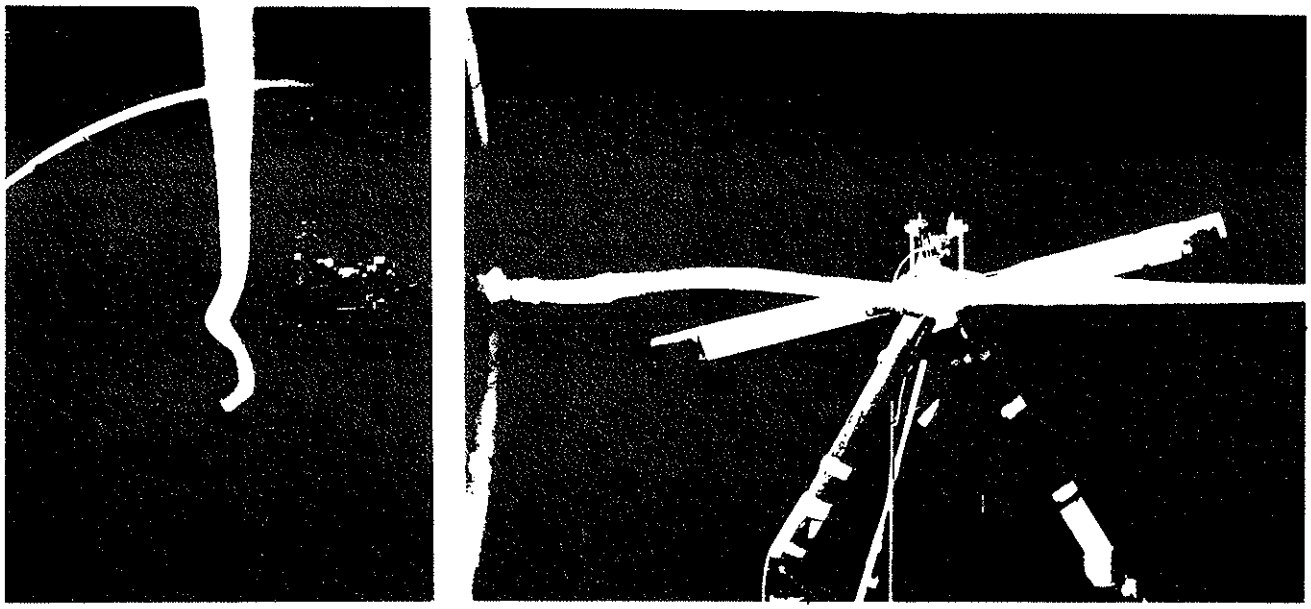

Fig. 11 'Long spiral'

In lifting cases, an additional axial displacement of the actively distorted vortex segments took place by the rotor downwash, especially for higher axial distances z_V between the vortex and the rotor area. The wave length of the spiral was larger than in the non-lifting case as can be seen in Fig. 11; we call this a 'long spiral'.

To get quantitative data of the trajectory disturbances, the flow photographs were analyzed by the image processing unit. The spiral wave length λ and its amplitude A (or spiral radius) were measured as comparable parameters. Fig.12 gives a scheme of the analyzing technique. The limited number of computer screen dots led to errors up to 8% for the amplitudes and 5% for the wave length.

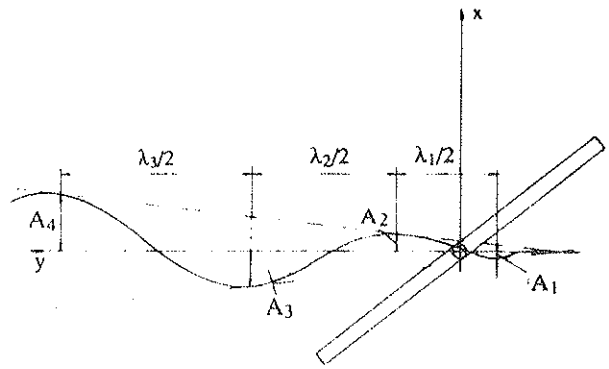

Fig. 12 Analyzing scheme

The discussion of the influence of the various test parameters starts with the axial distance z_V between the vortex axis and the rotor area. Fig. 13 shows the decrease of amplitudes A of the vortex spiral with increasing interaction distances z_V. It is remarkable that negative z_V-values (vortex above the rotor) show the largest amplitudes. Unfortunately, measurements above the rotor

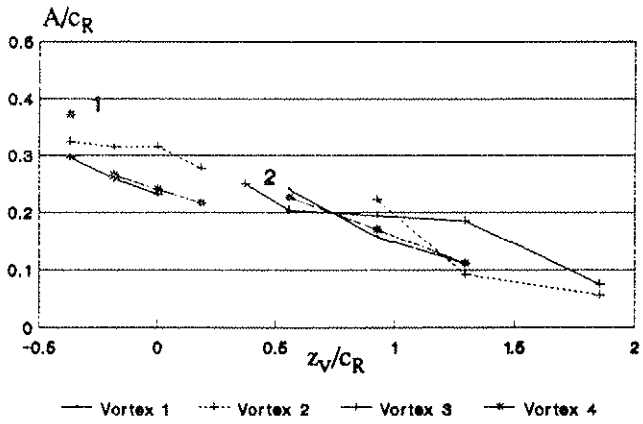

Fig. 13 Spiral amplitudes (nonlifting case)

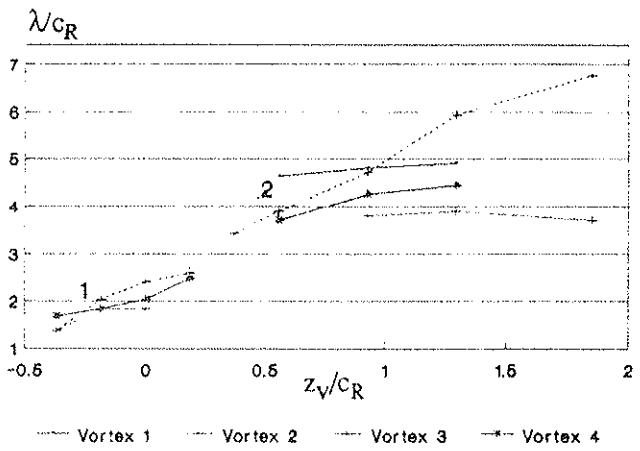

Fig. 14 Spiral wave lengths (nonlifting case)

were made only for small distances z_V up to now; the results require some more investigations in this configuration. While the amplitudes decrease with z_V, the

wave lengths increase (Fig. 14). In all cases, a maximum wave length can be found which is constant for larger z_V. The wave lengths and amplitudes show only small differences for the various vortices. Only the weak vortex 3 had relatively high wave lengths and amplitudes for larger distances ($z_V/c_R>1$). For z_V-values larger than 0.5 c_R, the wave length can be so large, that parts of it were affected by the second blade too. This is indicated by a (2) in the figures 13 to 16. Fig. 15 and 16 show the amplitudes and wave lengths in the lifting rotor case. Comparing these results with those of the non-lifting case (Fig. 13 and 14), it can be seen that for close interactions ($z_V/c_R<1$) the thrust does not influence the vortex trajectory very much. But, for larger interaction distances, the amplitudes and wave lengths are higher. Additionally the trajectory distortions are extended to larger distances z_V (up to $z_V/c_R=4$) in case of a lifting rotor. This can be explained as an effect of the rotor downwash. The more stable vortex 1 shows smaller amplitudes than vortex 2. Investigating the other parameters, it was found that smaller advance ratios cause smaller amplitudes and wave lengths, while a higher rotor speed is connected with longer wave lengths and slightly smaller amplitudes.

In the oblique interaction case it was not possible to examine the wave length with the required accuracy. Therefore, the angle of deflection γ (see Fig. 17) and the amplitude A were chosen as the scale of distortion.

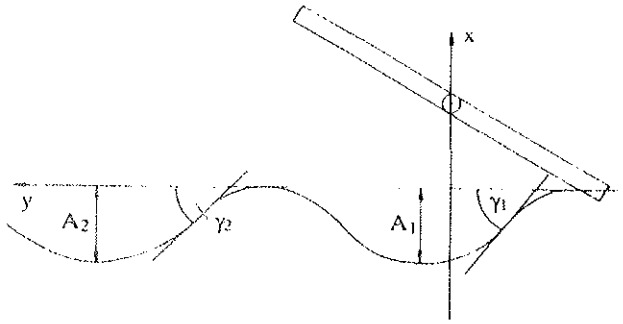

Fig. 17 Analyzing scheme for oblique case

Fig. 18 shows that the angle γ decreases rapidly with increase of the interaction distance z_V. The amplitudes are reduced as well with larger z_V (Fig.19); $z_V/c_R=-0.37$ shows maximum values (for larger distances above the rotor further measurements have to be conducted in future). The trajectory distortions are mainly caused by

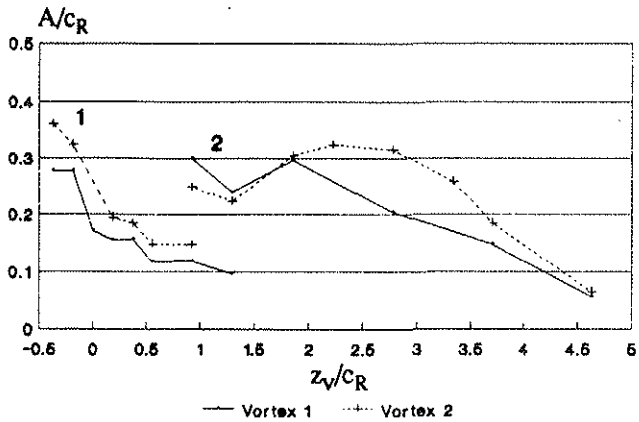

Fig. 15 Spiral amplitudes (lifting case)

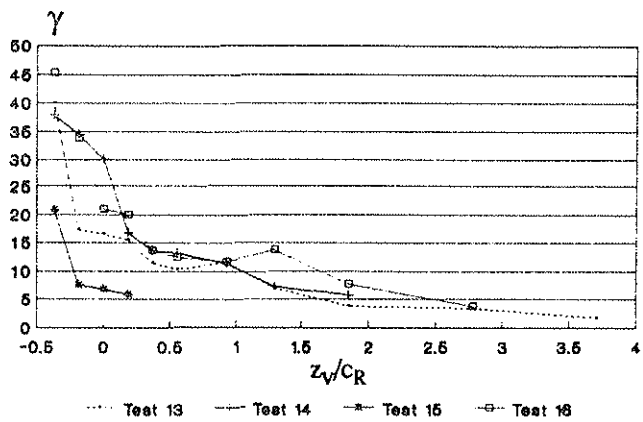

Fig. 18 Angle of deflection

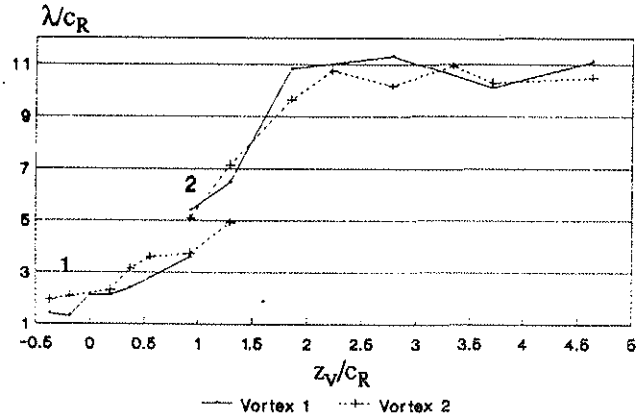

Fig. 16 Spiral wave lengths (lifting case)

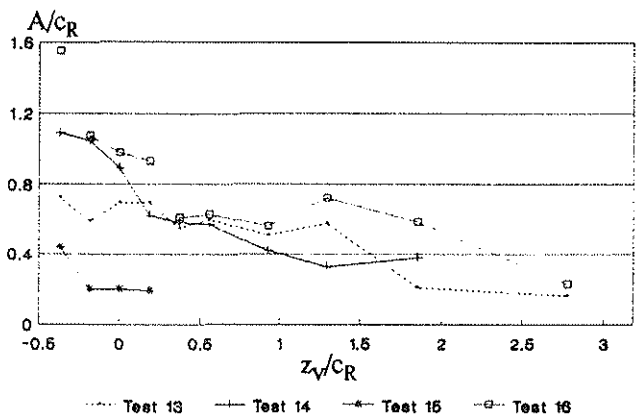

Fig. 19 Spiral amplitudes (oblique case)

rotor downwash, especially close interactions are strongly influenced in this case. As the non-lifting case (Fig. 15) shows the lowest values for A and γ, there are reasons for the assumption that the tip vortices of the rotor blades have an important influence in the oblique interaction case with a lifting rotor. The blade tip vortices induce velocities in the downwash direction. This induction acts for the oblique case over a longer period of time on the interacting vortex and can cause the 'flat spiral' with a higher amplitude normal to the rotor area.

Only a slight influence of the rotor speed could be found (test 13 compared to 14). The vortex stability seems to have more influence (the unstable vortex 2 in test 16 has the highest amplitudes).

3. 2. Velocity profiles

Additionally to the parameters of the spiral motion of the interacting vortices, it is of interest to get informations about the vortex velocity profiles. As mentioned above, the profiles of the tangential and axial velocities have been measured in several planes by split fiber probes. The maximum tangential velocity, the axial velocity defect δ - equal to (V_∞ - $V_{ax\ min}$) - and the vortex core radius can be considered as characteristic parameters of these profiles.

Fig. 20 shows the dimensionless tangential velocity V_{tan}/V_∞ plotted versus the dimensionless vortex radius r/c_W for various times t past interaction. Here, a parallel interaction case of vortex 1 with a lift generating rotor at V_∞ = 20 m/s (test 10) and z_V = 50 mm was considered.

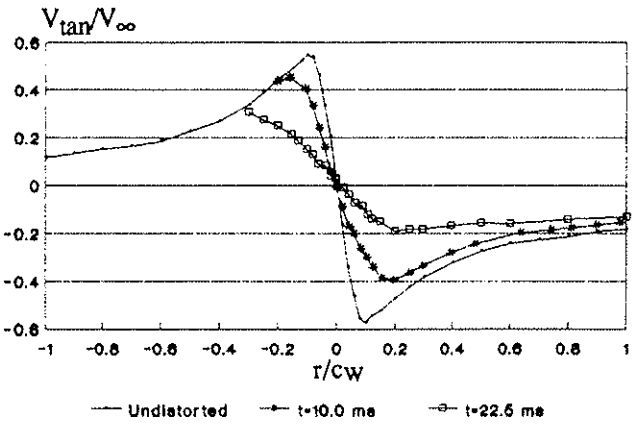

Fig. 20 Tangential velocity profiles

At the interaction time t = 0 the investigated segment of the vortex was located at r/R = 0.94 and ψ = 180°. The probe was traversed normal to the rotor disc. For the different times t past interaction, the measurement position of the profiles was moved with the flow, having the speed of V_∞ = 20 m/s. That leads, e.g. for t = 22.5 ms, to a measurement plane which is 0.04 R upstream the rotor center; the rotor blade has moved 125° in the direction of rotation. A substantial reduction of the tangential velocity connected with a considerable increase of the vortex core radius due to BVI could be concluded from analyzing Fig. 20. But, the fact that the probe is traversed in a fluctuating vortex leads to a smoothing of the velocity profiles, which are averaged over about 30 revolutions of the rotor. In this case, the above mentioned triggering of the plotted velocity data by the rotor did not work with enough accuracy. By analyzing unsteady velocity data of V_{tan}, the maximum values of the tangential velocity reached always nearly the same high values as for the undistorted vortex. That means that in Fig. 20 the plotted reduction of V_{tan} and the increase of the core radius is caused by the used measurement technique. In chapter 3.1 was concluded that a forced meandering of the interacting vortex in form of a spiral takes place. But this should not influence the velocity profiles as shown in Ref. 7.

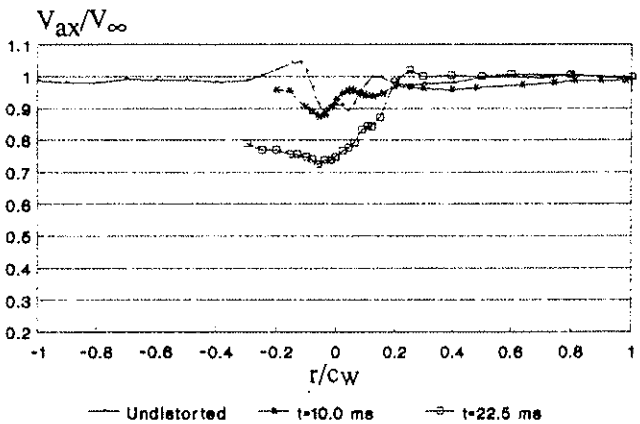

Fig. 21 Axial velocity profiles

For the same test number, the profiles of the axial velocities are given in Fig. 21. With a meandering vortex these profiles should be similar to the undistorted vortex. But Fig. 21 shows an increasing deficit δ with growing time t. This takes place obviously on the axis of the vortex spiral and can not be explained by an averaging process during the measurements as above. Here a possible explanation is, that the vortex itself induces an upstream axial velocity in the center part of the spiral (Ref. 7). This induced velocity grows when the wave length of the spiral is decreased and the amplitude is increased. Such a behaviour of the spiral can be seen for the present test number in Fig. 22 (it shows a photographic recording of one picture of a video movie). The probe position for t = 22.5 ms is in that region where the spiral shows the increased pitch.

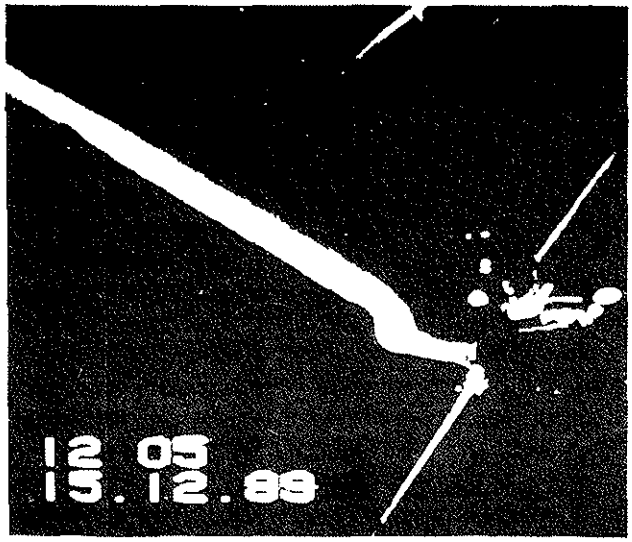

Fig. 22 Vortex deformation

In some cases (all at a low separation distance z_V) a local bursting of the interacting vortex was observed. This is shown in the lower picture of Fig. 9 with a z_V = +10 mm. After a sharp displacement of the vortex during interaction (upper picture of Fig. 9), a strong distortion can be seen in the middle picture followed by a vortex bursting in form of a spiral having high pitch. Another example, showing vortex bursting, is given in Fig. 23 with a z_V = -10 mm. This bursting has not yet been investigated in detail. Because such a bursting reduces the flow distortions downstream, a special investigation of this effect is planed for the future.

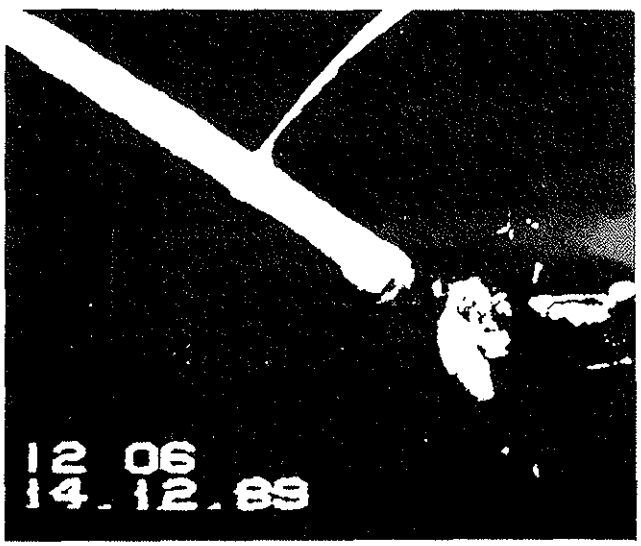

Fig. 23 Vortex bursting

4. Conclusions

In this paper the special effect of BVI on the deformation of the vortex path as well as a modification of its internal structure is investigated. The knowledge of these phenomena seems important because the distorted vortex segments can interact for several times with the main rotor blades as well as with the tail rotor blades. To simulate the BVI for a helicopter in forward flight, the interacting vortex was generated by a special wing arrangement. This experimental setup allowed an easy measurement of the vortex location, structure and strength before and after the interaction. Vortex trajectory distortions were recorded by vapor visualization and photo/video technique. The distributions of the axial and tangential velocities inside the interacting vortices were investigated by measuring the velocity profiles using split fiber probes.

The influence of several parameters has been observed during a wind tunnel campaign. It was found that a forced meandering took place due to BVI and the straight trajectory of the undistorted vortex was turned into a spiral motion. The meandering has different reasons (see below) and leads to a spiral motion which is generated by self-induction of the vortex.

- In the case of parallel interaction (vortex trajectory parallel to the leading edge of the blade, see e.g. Fig. 7) the circulation at the blade is changed with time. This causes a trailing vortex sheet whose induced velocities lead to a displacement of the interacting vortex segments parallel to the rotor area (see Fig. 10). That is the origin of the meandering and takes place for a rotor with and without lift.

- If the blades generate lift, the rotor downwash leads to a displacement of the interacting vortex normal to the rotor area.

- Increasing the separation distance z_V between the vortex axis and the rotor disc for a non-lifting blade, the amplitude A of the generated vortex spiral decreases and simultaneously the wave length increases. A vortex with a low strength has larger amplitudes and wave lengths.

- If the vortex interacts with a lifting blade, the values of the amplitudes and wave lengths of the vortex spirals are nearly the same as in the non-lifting case for z_V being small (up to about 1.5 blade chord lengths). Downwash, however, expands the z_V-range where the vortex trajectory is influenced up to values of 4.5 blade chord lengths. In this range the wave lengths are rather long.

- In the case of oblique interaction (flow visualization in Fig. 8) the blade tip vortices of the rotor blades can influence the vortex displacement in a significant way. The tip vortices induce velocities in downwash direction. In the oblique case these inductions act on the interacting vortex for a longer period of time and can cause a ´flat spiral´ with higher amplitudes normal to the rotor area. In the non-lifting case the amplitudes are of the same level as in the case of parallel interaction. But, when tip vortices are generated in the lifting case, these amplitudes are increased with a factor of about 3 (Fig. 19).

- The distribution of the tangential and axial velocities inside the interacting vortex, which is meandering in form of a spiral, have been measured by split fiber probes. In such a vortex the tangential velocity profiles are nearly identical with those in an undistorted vortex. But, the axial velocities near the center of the spiral can be decreased. It is assumed, that here the vortex itself induces axial velocities against the flow direction especially in those cases where the spiral has regions with increased pitch.

- For very close interaction (z_V in the range up to 0.2 c_R) not only the vortex trajectory is influenced by BVI but the vortex structure is also changed. Flow visualizations show that a bursting of the interacting vortex may be induced in form of a short spiral with high pitch (Fig. 9 and 23 show the vortex bursting).

- For the future it is planned to investigate especially those cases where a vortex bursting is to be expected. It is known, that the tangential and axial vortex velocities downstream the burst become very low. This leads to a decrease of the unsteady blade pressure fluctuations due to BVI. Therefore these cases are most interesting ones.

5. Acknowledgements

This research program was sponsored by the DFG in the SFB 25 ´Wirbelströmungen in der Flugtechnik´. The author would like to thank Dr. G. Neuwerth for hours of helpful discussion. The figures were prepared by R. Göke and U. Heinz.

6. References

(1) Neuwerth G., Müller R.H.G., 'Pressure fluctuations on rotor blades generated by blade-vortex-interactions', 10th European Rotorcraft Forum (ERF) 1984, and Vertica 1985, Vol. 9, No. 3

(2) Müller R.H.G., Staufenbiel R., 'The influence of winglets on rotor aerodynamics', 12th ERF 1986 and Vertica 1987, Vol. 2, No. 4, pp. 601-608

(3) Caradonna, F.X., Laub, G.H., Tung, C., 'An experimental investigation of the parallel blade vortex interaction', 10th ERF 1984

(4) Tung, C., Pucci, L., Caradonna, F.S., Morse, H.A., 'The structure of trailing vortices generated by model rotor blades', 7th ERF 1981

(5) Leibovich, S., 'Vortex stability and breakdown: Survey and extension', AIAA 1983, Vol. 22, No. 9, pp. 1192-1206

(6) Leibovich, S., Stewartson, K., 'A sufficient condition for the instability of columnar vortices', Journal of Fluid Mechanics 1983, Vol. 126, pp. 523-530

(7) Vitting, T., Staufenbiel, R., Coors, D., 'Geschwindigkeitsmessungen und Stabilitätsuntersuchungen an aufplatzenden Randwirbeln', to be published in Z. Flugwiss. u. Weltraumforschung